Simulation of Low-Noise Low-Power CMOS Readout Front-End Electronics for Mammo- and Dentography

V. Barzdėnas, R. Navickas

Computer Engineering Department, Vilnius Gediminas Technical University,
Naugarduko str. 41, LT-03227 Vilnius, Lithuania, phone: +370 684 51453; e. mail: vaidotas.barzdenas@el.vtu.lt

Introduction

Active pixel detectors (APD) have been widely used as reliable devices for high precision particle detection in particle physics experiments and in medical applications [1-4]. If high spatial resolution, radiation hardness, mechanical stability, long term reliability, robustness, flexibility in the technology, eventually low cost is desired, then an array size of pixel detectors, material of APD and read-out electronics should be sought. In particular, the low power and high integration of the CMOS 0.24 μm technology make it an attractive choice for high-resolution APD-based imaging detection systems for medical diagnostics like mammography and dentography.

Recent studies on deep sub-micron CMOS technologies have triggered interest for applications where highly integrated analog front-end electronics is required.

The scaling of the power supply down to 2 V reduces the available dynamic range, but the gain in signal-to-noise ratio at a given dissipated power makes these choice attractive compared to older technologies [4-5].

In this paper, the simulation results obtained with Charge Sensitive Preamplifier (CSP) for medical imaging implemented in CMOS 0.24 μm technology are reported.

Readout Front-End Electronics

The charge created by the interaction of X-ray photons in the sensor is very small (a 10 keV photon will produce 2800 charge carriers at the preamplifier) and has to be amplified in a low-noise circuit before any further signal processing. The signal induced on the electrodes (In bump) of the sensor is transferred to the readout chip, where it is integrated in a charge sensitive amplifier (CSA). CSA built of two basic blocks: charge sensitive preamplifier (CSP) and pulse shaping amplifier (See Fig. 1) [6-9]. Thus, the analogue part of an event counting pixel cell starts with the preamplifier followed by a pulse shaping amplifier. The preamplifier design is critical since it should match the detector interface. The circuit should be fast with low noise performance.
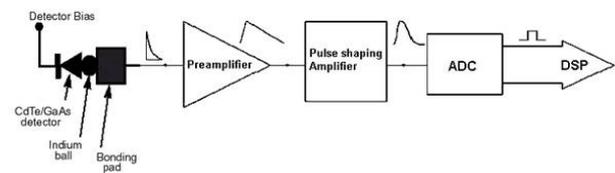

Fig. 1. Block diagram of a generalized analog pulse-processing channel (ADC – Analog-Digital Converter, DSP- Digital Signal Processing)

The preamplifier output signal is in many cases amplified and shaped in a subsequent stage, called the shaper. In its simplest form it is constructed as a RC-CR filters that shapes the signal into a semi-Gaussian pulse form. The shaper optimizes the signal-to-noise ratio and band-limits the signal to remove low-frequency noise. The preamplifier and the pulse shaping amplifier are often referred to as the front-end or readout chip. But usually pulse shaping amplifier is not used to minimize power consumption [4, 7-9]. The last element in the chain is the ADC, which converts the output of the pulse shaping amplifier in a digital number for further processing in the data acquisition.

Modeling of CMOS Charge Sensitive Preamplifier

The CSP configuration and the input transistor size and bias set the fundamental limit of the overall system noise and power dissipation.

Simulation has been performed with PSPICE simulator using the BSIMV3.3 parameters of the MOSIS CMOS SCN 0.24 μm [10]. The well known principle of the CSP is shown in Fig. 2. It consists of an operational amplifier with a feedback capacitor C_{fb} which is discharged by an external resistor R_{fb}. The value of this resistor is typically in the Megaohm range for a minimal parallel noise contribution. To reach that high resistor value using MOS transistors the transistor should be operated in its non-saturation region, which is a challenging objective since its Rds is subject to fluctuations due to the variations

in its threshold and bias conditions [11-14]. The detector represented by its capacitance C_{det}, is connected to the inverting input. CSP giving rise to a voltage step at the output with amplitude of Q_{in}/C_{fb}. The output voltage at an input charge Q is

$$V_{out} = -\frac{Q_{in}}{C_{fb} + \frac{C_{det} + C_{inp} + C_{fb}}{A}} = -\frac{Q_{in}}{C_{fb}}; \quad (1)$$

where C_{inp} represents the input capacitance of the amplifier, usually dominated by the input transistor, A - gain of operational amplifier (OPAM). The feedback capacitance is inversely proportional to the voltage gain of the system.
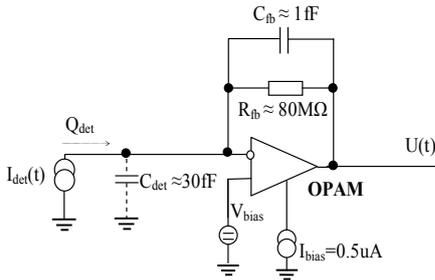

Fig. 2. Block diagram of the preamplifier

The main design parameters are given in Table 1.

Table 1. Main design parameters of the preamplifier

Power supplies	V_{dd}= +1.2 V
Bias voltage of preamplifier	V_{bias}= 400 mV
Bias current of preamplifier	I_{bias}= 0.5 µA
Input transistor (T1) dimension	W/L= 1.2 µm /0.24 µm
Feedback capacitance	C_{fb}=1 fF
Capacitance of semiconductor detector	C_{det}=30 fF
Feedback resistance	R_{fb}=80 MΩ
Shaping time	τ_p=45 ns
Power consumption	P_{tot}= 1.2 µW
ENC	115 ē
Linearity	3% (1 kē…10 kē)
Gain	115 mV/kē

The simulated transient curve is presented in Fig. 3, a for an input-current pulse corresponding to 1000 ē (0.16 fC) charge signal. From this figure, a conversion gain (charge-to-voltage gain) of 115 mV/kē and a peaking time of 45 ns have been obtained, for detector capacitance C_{det}=30 fF. A near-Gaussian pulse shape is produced, yielding optimum signal-to-noise characteristics [3].
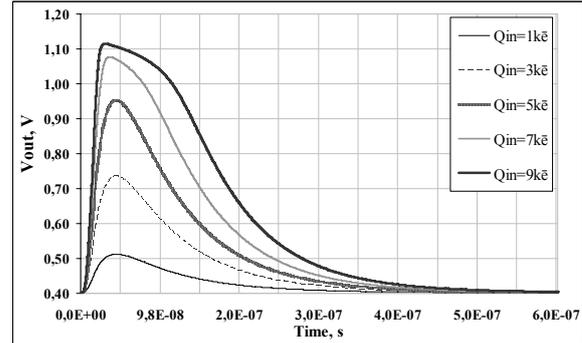
The preamplifier output signal is usually a semi-Gaussian pulse form with an exponential a long time constant decay. Decay of the signal is proportional to exp(-t/80ns) (Fig. 3 a),

$$\tau_D = R_{fb} \cdot C_{fb} = 80 ns; \quad (2)$$

where τ_D – return to baseline time.
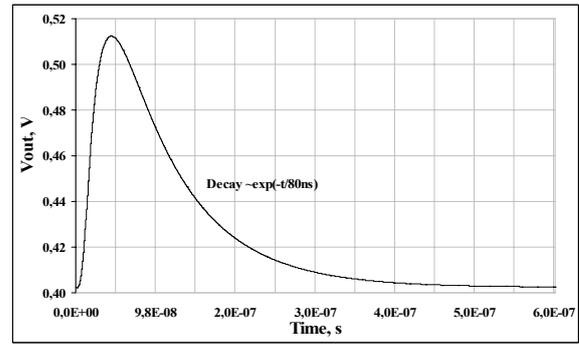
a)

b)

Fig. 3. Real signal response of the preamplifier: a) The preamplifier output signal with decay time (Q_{in}=1 kē, C_{det}=30 fF); b) Simulations of the CSP output waveform for five values of injected charge (C_{det}=30 fF)

Fig. 3, b shows the simulated pulse response of CSP. The input signals are charge steps 1 kē…9 kē with applied to a 30 fF capacitor at the preamplifier input.

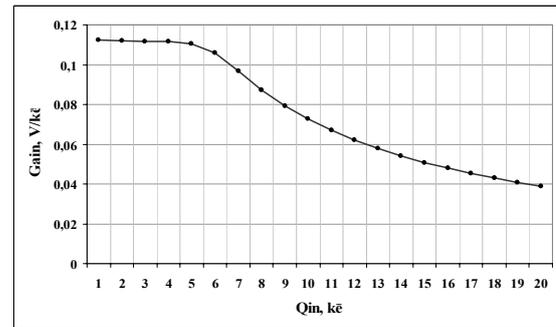**Fig. 4.** Gain versus of the input charge (C_{det}=30 fF)

Gain versus of the input charge is shown in Fig. 4. CSP gain, when the input charge 1...20 kē, is about 112...40 mV/ kē, respectively (when the temperature is 27 °C).

CSP is often used in surrounding ambience with low temperature. Thermal analysis simulated in the range – (-120 ºC) ÷ (+120 ºC) shows changes of not more than 20 ns in the decay time and less than 10% of the output signal amplitude (Fig. 5, a). Gain at the temperature -120 °C decreases from 125 mV/kē up to 99.2 mV/kē when temperature is equal +120 °C (Fig. 5, b).
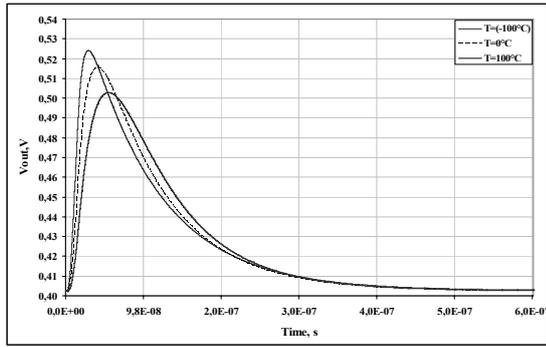
a)
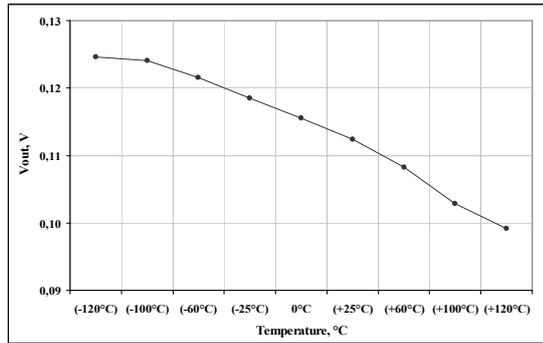
b)

Fig. 5. Results of temperature simulation (Q_{IN}=1kē): a) Real signal response of the preamplifier for different temperatures; b) Gain as a function of temperature

Fig. 6 shows the peaking time versus the detector capacitance. The simulation shows a peaking time of 14 ns at of 0 pF input capacitance and a weak dependence with the input capacitance.
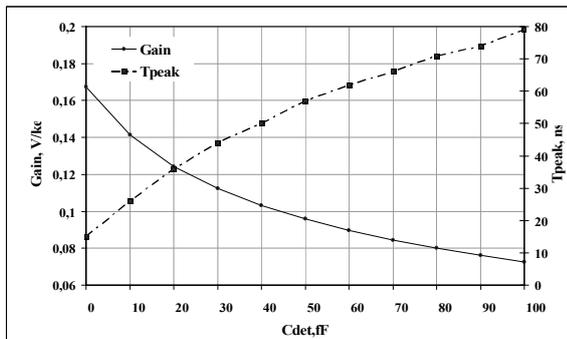

Fig. 6. Preamplifier peaking time and gain versus the input capacitance (Q_{in}=1 kē)

The expected peaking time (Cdet=30 fF) for the preamplifier alone is about 45 ns. The deterioration of the preamplifier speed is due to the increase of capacitance in the coupling with the discriminator stage.

The preamplifier showed a good linearity up to 6 kē for an input capacitance of 30 fF, as shown in Fig. 7.

Information lost in the detector cannot be restored later; therefore the noise of the detector has to be minimized. It is useful to express the noise sources as an equivalent noise charge (ENC) at the preamplifier input. Clearly, the ENC depends on the characteristics of both the

charge sensitive preamplifier. The expression for the equivalent noise charge for the noise sources mentioned
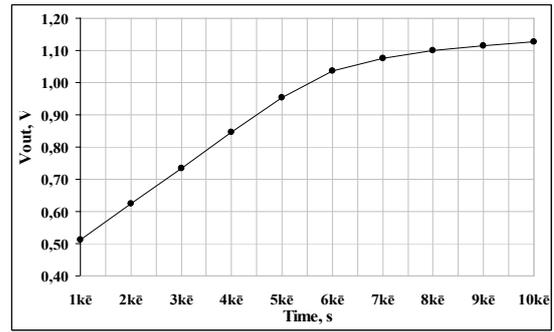

Fig. 7. Analog output signal as a function of the input charge

have been calculated in [8, 11, 14]. The series and parallel noise sources as well as flicker noise were accounted for to simulate total ENC of the CSP. Some parameters of total ENC depend on assigned constraints such as the detector capacitance, the time integration, the gate capacitance of the input transistor, the drain-source current and the leakage current of the detector.
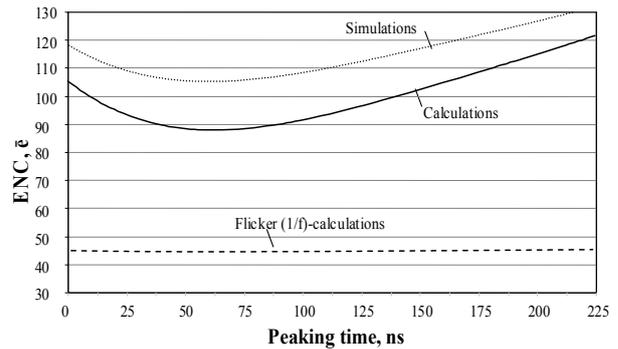

Fig. 8. ENC as a function of peaking time: results of simulation and calculations

Fig. 8, a presents the simulation results of the ENC contributions as a timing resolution. Minimum equivalent noise charge is obtained at the shaping time where the current (parallel noise sources) and voltage noise (serial noise sources) contributions are equal. The maximum allowable peaking time is in practice constrained by other design factors, as for example the maximum pulse-hit frequency that the circuit should be able to handle. For short peaking times the dominant noise is the serial noise, for long peaking times - parallel noise. This function is quadratic, concave with one minimum, which is adequate for ENC minimum, ENC = 105 ē, when τ_p= 75ns.

Flicker noise of CMOS transistors is dominated by 1/f noise up to relatively high frequencies of the order of several tens of kilohertz [9, 11]. The flicker noise is independent of peaking time (Fig. 8.) and the ENC$_{1/f}$ = 45 ē. Calculations and computer simulations show that a detector resolution as low as <105 noise electrons can be obtained, congruity is more than 85%.

Conclusions

Computer simulation was carried out by PSPICE simulator using the BSIMV3.3 parameters of the MOSIS CMOS SCN 0.24 μm and has been shown to simulate charge sensitive preamplifier together with associated semiconductor detector for various chapping times, detector capacitances and inputs charges. The advantage of this design is its low-noise level, a high speed and a high gain with very low-power consumption 1.2 μW for the whole preamplifier. The preamplifier has unipolar response with peaking time about 45 ns and the gain is 100mV – 125 mV/kē and equivalent noise charge ENC less 110 ē, when input charge is 1…20 kē and detector capacitance is equal 30 fF. Noise simulations indicate an excellent performance and agree with noise calculations based on the models for 0.24 μm CMOS technology.

References

1. **Bardelloni G., Bertolucci E., et al.** A new read-out system for an imaging pixel detector // in Proc. Conf. Rec. IEEE Nuclear Science Symp. Medical Imaging Conf., Lyon, France, Oct. 15–20, 2000. –P. 57–60.
2. **Novelli M., Amendolia S.R., Bisogni M.G., et al**. Semiconductor pixel detectors for digital mammography // NUCLEAR INSTRUMENTS & METHODS IN PHYSICS RESEARCH. SECTION A-ACCELERATORS, 2003. –Vol. 509. –P. 283–289.
3. **Barzdėnas V., Navickas R**. GaAs krūviui jautrių stiprintuvų skaičiavimas ir analizė // Elektronika ir elektrotechnika. – Kaunas: Technologija, 2005. – Nr. 6(62). – P. 26–30.
4. **Lopart X., Campbell M., San Secundo D. and Pernigotti E.** Medipix2: a 64k pixel readout with 55 μm square elements working in single photon counting mode // IEEE Trans. Nucl. Sci., 2002. –Vol.49 (5). –P. 2279–2283.
5. **MEDIPIX** project. www.cern.ch/MEDIPIX
6. **Navickas R., Morozov V.** Design of Charge Sensitive Amplifiers in a GaAs MESFET Technology // Information Technology and Control. – Kaunas: Technologija, 2000. –Nr. 1(14). – P. 60–64.
7. **O'Connor P., De Geronimo G.** Prospects for charge sensitive amplifiers in scaled CMOS // Nucl. Instrum. Methods, 2002. –Vol. A480, no. 2. – P. 713–726.
8. **Krummenacher F.** Pixel detectors with local intelligence: An IC designer point of view // Nucl. Instrum. Methods Phys. Res., 1991. – Vol. A305. – P. 527–532.
9. **Sansen W. M. C., Chang Z. Y.** Limits of low noise performance of detector readout front ends in CMOS technology // IEEE Trans. CircuitsSyst., Nov. 1990. –Vol. 37. – P. 1375–1382.
10. **MOSIS,** www.mosis.org
11. **De Geronimo G. O'Connor P.** A CMOS detector leakage currentself-adaptable continuous reset system: Theoretical analysis // Nucl. Instrum. Methods, 1998. –Vol. A421. – P. 322–333.
12. **Enz C. C., Krummenacher F., Vittoz E. A.** An analytical MOS transistor model valid in all regions of operation and dedicated to lowvoltage and low-current applications // Anal. Integ. Circuits Signal Processing, 1995. –Vol. 8. – P. 83–114.
13. **Binkley D. M., Puckett B. S., Casey M. E., Lecomte R., Saoudi A.** A power efficient, low-noise, wideband, integrated CMOS preamplifier for LSO/APD PET systems // IEEE Trans. Nucl. Sci., May 2000. –Vol. 47. – P. 810–817.
14. **Tsividis Y. P., Suyama K.** MOSFET modeling for analog circuit CAD: Problems and prospects // IEEE J. Solid-State Circuits, Jan. 1994. –Vol. 29. – P. 210–216.

V. Barzdėnas, R. Navickas. Simulation of Low-Noise Low-Power CMOS Readout Front-End Electronics for Mammo- and Dentography // Electronics and Electrical Engineering. – Kaunas: Technology, 2006. – No. 6(70). – P. 75–78.
Simulation of differential charge sensitive amplifiers (CSA) for hybrid pixel detectors on CMOS technology for high energy particle physics and for mammography, dentography has been performed with PSPICE simulator using the BSIMV3.3 parameters of the MOSIS CMOS SCN 0.24 μm. Charge sensitive preamplifier when input charge 1…30 kē and input capacitance equal 0...100 fF has the following main electrical parameters: 167...73 mV/kē gain and low power consumption 1.2 μW/channel. The preamplifier has unipolar response with peaking time about 15...79 ns. A near-Gaussian pulse shape is produced, yielding optimum signal-to-noise characteristics, and equivalent noise charge of input (ENC) less 105 ē. Thermal analysis simulated in the range T= -120…+120ºC shows changes of not more than 20 ns in the decay time and less than 10% of the output signal amplitude. Ill. 8, bibl. 14 (in English; summaries in English, Russian and Lithuanian).

В. Барзденас, Р. Навицкас. Моделирование малошумящих и маломощных КМОП первоначальных регистрирующих систем в маммографии и дентографии // Электроника и электротехника. – Каунас: Технология, 2006. – № 6(70). – С. 75–78.
Для точечных детекторов в медицинских исследованиях в дентографии и маммографии и для исследования физики высокоэнергетичных элементарных частиц основные параметры зарядочувствительного предусилителя (ЗЧУ), основанного на КМОП технологии, получены моделированием при помощи программного пакета PSPICE, используя КМОП 0.24 мкм транзисторные BSIMV3.3 модели компании MOSIS. Для моделирования ЗЧУ были установлены такие основные технические требования: входная ёмкость точечных детекторов – $C_{дет}$ изменялась от 0 до 100 фФ, входной сигнал $Q_{вх}$ - от 1 до 30 Kэ, рабочая температура - от -120 °C до +120 °C. Были получены эквивалентный шумовой заряд менее 105 электронов, коэффициент преобразования от 167 мВ/Кэ до 73 мВ/Кэ, длительность фронта выходного импульса от 15 нс до 79 нс при потребляемой мощности 1.2 мкВт. Ил. 8, библ. 14 (на английском языке; рефераты на английском, русском и литовском яз.).

V. Barzdėnas, R. Navickas. Mažų triukšmų ir mažos galios KMOP pirminių dalelių registravimo sistemų mamografijoje ir dentografijoje modeliavimas // Elektronika ir elektrotechnika. – Kaunas: Technologija, 2006. – Nr. 6(70). – P. 75–78.
Mažų triukšmų ir mažos galios diferencinio krūviui jautraus priešstiprintuvio (KJP) modeliavimas atliktas PSPICE programų paketu, naudojant kompanijos MOSIS 0,24 μm technologijos KMOP tranzistorius. Visi modeliavimo rezultatai gauti esant įvairioms KJP darbo sąlygoms: kai jutiklių talpų C_{det} diapazonas buvo 0...100 fF, perdavimo koeficientas keitėsi nuo 167 iki 73 mV/kē, o sistemos registracijos trukmė τ_p = 15...79 ns. KJP buvo modeliuojamas plačiame įejimo signalų Qin=1...30 kē ir veikimo temperatūrų T= -120...+120 ºC diapazone. Gauta labai maža KJP vartojamoji galia, kuri neviršija 1,2 μW/vienam kanalui, o ekvivalentinis triukšmų krūvis (ENC) priešstiprintuvio įejime yra mažas ir lygus 105 ē. Il. 8, bibl. 14 (anglų kalba; santraukos anglų, rusų ir lietuvių k.).